CHARACTERIZATION OF THE MARTIAN MESOSPHERE BY LMD-MGCM SIMULATIONS COMPARED TO NOMAD/TGO OBSERVATIONS.

F. González-Galindo, *Instituto de Astrofísica de Andalucía-CSIC, Granada, Spain (ggalindo@iaa.es)*, **M.A. López-Valverde, A. Brines, A. Modak, A. Stolzenbach, B. Funke, J.J. López-Moreno,** *Instituto de Astrofísica de Andalucía-CSIC, Granada, Spain*, **F. Forget, E. Millour,** *Laboratoire de Météorologie Dynamique, IPSL, Paris, France*, **F. Lefèvre, M. Vals, F. Montmessin,** *LATMOS, Paris, France*, **M. Patel,** *Open University, Milton Keynes, UK*, **G. Bellucci,** *Istituto di Astrofisica e Planetologia, Italy*, **A.C. Vandaele,** *BIRA, Brusels, Belgium*.

Introduction

Since the beginning of the 21st century, many different missions have provided unvaluable information about the Martian atmosphere, including its seasonal and geographical variability. So, remote sounding by orbiters such as Mars Global Surveyor and Mars Express allowed for a good characterization of the dust, water and CO_2 cycles in the lower atmosphere, as well as their effects on the temperature structure (Smith, 2004; Montmessin et al., 2017). In situ measurements by landers and rovers have unveiled the meteorological structure near the surface of the planet (e.g. Savijarvi et al., 2019). The thermosphere/ionosphere region, as well as the magnetosphere and its interaction with the solar wind, have been explored by Mars Express and specially the MAVEN mission by a combination of remote sounding and in-situ measurements (e.g. Bougher et al., 2017).

The Martian mesosphere, and in particular the upper mesosphere, above about 80 km from the surface, remains poorly explored in comparison with the troposphere and the thermosphere/ionosphere. Remote sounding by the Mars Climate Sounder instrument on board Mars Reconnaissance Orbiter have allowed systematic measurements of the mesospheric temperature, but only below 80 km (McCleese et al., 2010). Stellar occultations by SPICAM on Mars Express (Forget et al., 2009) and IUVS on MAVEN (Gröller et al., 2018) have provided CO_2 density and temperature measurements in the upper mesosphere, mostly on the night side, but far from a complete coverage due to the limitations of the stellar occultation technique. Observations of the mesospheric CO_2 clouds mostly by Mars Express and MAVEN have been used to gain insight into the temperature and winds in the mesosphere (Määttänen et al., 2010, González-Galindo et al., 2011). The analysis of UV atmospheric emissions by Mars Express and IUVS/MAVEN has also supplied information about the dynamical structure of the mesosphere (Gagné et al., 2013, Schneider et al., 2020). Many of these observations have been interpreted thanks to the use of Global Climate Models (GCMs, e.g. González-Galindo et al., 2011). However, the scarcity of observations of the Martian mesosphere, and in particular of the composition and temperature variability in the upper mesosphere, has not allowed yet for a complete validation of the predictions provided by GCMs.

Observations by the NOMAD and ACS instruments on board the ExoMars Trace Gas Orbiter mission (TGO in what follows) are starting to fill this gap by providing measurements such as the abundance of mesospheric water and the effects of global dust storms (Vandaele et al., 2019; Belyaev et al., 2021; Brines et al., 2022), the CO variability (Modak et al., 2022) or the temperature and density structure (López-Valverde et al., 2022). For the first time we have a set of diverse atmospheric parameters derived simultaneously with good vertical resolution and from a single instrument, which is ideal for model validation purposes.

In this work, we compare the predictions of the LMD-Mars GCM (LMD-MGCM) in the mesosphere with NOMAD observations, in order to validate the model and to gain insight into the physical processes at the origin of the observed structures.

IAA NOMAD datasets

The data used in this study haven been obtained by the NOMAD instrument using the solar occultation (SO) channel (and thus limited to the morning and evening terminators), and retrieved using the IAA retrieval scheme. This scheme uses the radiative transfer model KOPRA as a forward model and the Retrieval Control Program (RCP) to invert the vertical profile. More details about the IAA retrieval scheme can be found in López-Valverde et al. (2022). When applied to different NOMAD diffraction orders, the retrieval scheme provides measurements of the CO_2 density and temperature profiles, as well as profiles of CO and H_2O abundances. These have been analyzed in López-Valverde et al. (2022), Modak et al. (2022), and Brines et al. (2022), respectively, as well as in companion abstracts submitted to this conference. In the near future, additional species such as HDO will also be targeted.

LMD-MGCM

The LMD-MGCM version used in this study is the same version used to build the Mars Climate Database v5.3, including the formulations of the dust and water cycle

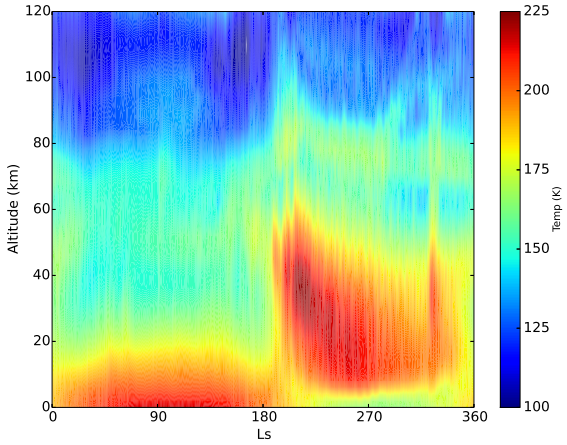

Figure 1: Seasonal variation of the temperature profiles predicted by the LMD-MGCM during MY34, at the morning terminator and a constant latitude of 45N

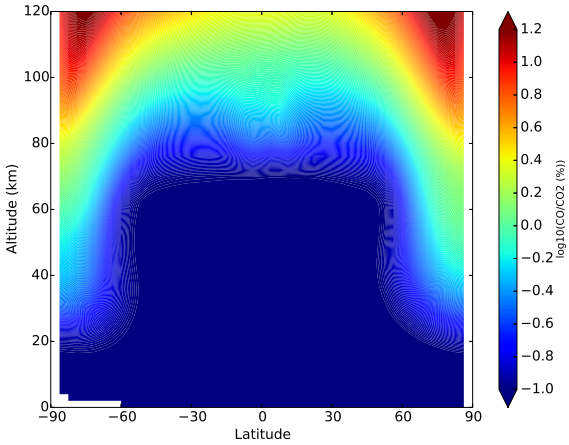

Figure 2: Latitudinal variation of the CO/CO_2 ratio profiles predicted by the LMD-MGCM at the morning terminator for Ls=180 and MY34

described in Navarro et al. (2014) and thermospheric processes described in González-Galindo et al. (2015).

We have performed simulations appropriate for Mars Years (MY) 34 and 35, using the observed dust abundance in the lower atmosphere given by Montabone et al. (2020) and the UV solar variability using the scheme described in González-Galindo et al. (2015).

We analyze the LMD-MGCM predictions in two different ways. First, for a direct one-to-one comparison with NOMAD measurements, the GCM results are extracted at the exact location and time of each of the NOMAD observations. Second, in order to provide a more general view of the atmospheric behavior at the terminators not limited to the NOMAD temporal and geographical coverage, a post-processing software developed at the LMD has been used to extract the model predictions at a fixed value of Solar Zenith Angle of 90 degrees, both in the morning and the evening terminators, at all latitudes and seasons.

Results

CO_2 density and temperature

Fig. 1 shows the variation with altitude and season of the temperature predicted by the LMD-MGCM in the morning terminator and in the mid latitudes of the Northern hemisphere for MY34. The effect of the global dust storm (GDS) starting shortly after L_s=180 in MY34 is clearly seen, producing an increase of temperature that is felt from the lower atmosphere to the top of the mesosphere. Note also the temperature increase produced by the regional dust storm around L_s=330. It is also noticeable the temperature peak predicted by the model at an altitude of around 80 km during the second half of the year.

While the starting phase of the MY34 GDS is not well covered by NOMAD observations, the retrieved temperature profiles show a maximum of temperature at around L_s=220, in agreement with the prediction of the model, as well as a temperature increase at the end of the year (López-Valverde et al., 2022). Interestingly, a temperature peak at around 80 km is also observed by NOMAD, although its seasonal extension seems to be more limited than in the simulations. However, a detailed comparison shows that the LMD-MGCM systematically overestimates the temperatures in the layers above 50 km (López-Valverde et al., 2022), suggesting deficiencies in the description of the radiative heating terms in the model and/or in the representation of tides or other dynamical processes affecting the temperature structure.

Regarding the CO_2 density, the strong seasonal variations observed by NOMAD are rather well captured by the model.

CO

Fig. 2 shows the latitudinal variation of the predicted CO abundance profiles during the equinox season. The CO mixing ratio increases with altitude, reaching values larger than 1% in the upper mesospheric layers, due to the effects of CO_2 photolysis producing CO in the upper layers, as well as the molecular diffusion of CO enhancing its abundance relative to CO_2 above the homopause.

A clear enhancement of the CO relative abundance

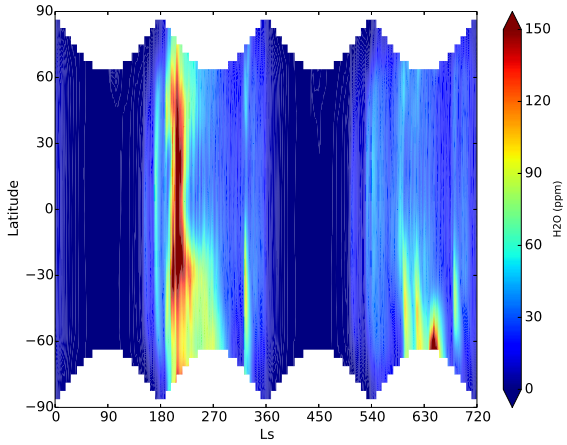

Figure 3: Seasonal and Latitudinal variation of the H_2O mixing ratio predicted by the LMD-MGCM at a constant altitude level of 60km, for the morning terminator and for MY34 (L_s=0-360) and MY35 (L_s=360-720

is predicted at both poles. This is the consequence of the structure of the meridional circulation at the equinox season, characterized by two symmetric Hadley cells transporting matter from the equator to both poles. This latitudinal variation of the CO abundance is supported by NOMAD observations, which show a similar enhancement in the high latitude regions during the equinox season (Modak et al., 2022).

A quantitative comparison with the CO abundances observed by NOMAD shows that the model tends to underestimate globally the CO relative abundance.

H_2O

Fig. 3 shows the latitudinal and seasonal variation of the H_2O relative abundance predicted by the LMD-MGCM in the morning terminator at a constant altitude of 60 km during both MY34 and MY35. It can be seen that during the aphelion season the water abundance is quite low, below a few ppms. The abundance increases in the perihelion seasons, reaching abundances of about 50 ppms for MY35. In MY34 the effect of the GDS is very clear, producing water abundances above 150 ppm.

Similarly, NOMAD observations show a strong increase of the mesospheric water abundance following the MY34 GDS, although observed values at 60 km exceed 200 ppm (Brines et al., 2022), larger than predicted by the model. An important difference is that the decay of the water abundance after the storm is stronger and faster in the observations than in the model prediction, so that the model significantly overestimates the mesospheric abundance until L_s=270.

On the perihelion season of MY35, on the other hand, the comparison of the mesospheric water abundance between NOMAD observations and the LMD-MGCM is quite good (Brines et al., 2022). This suggests that the overestimation during MY34 is probably caused by a misrepresentation of the vertical dust structure in the model during the MY34 GDS. A similar conclusion was obtained from the comparison of the LMD-MGCM water abundances with ACS observations (Vals et al., 2022).

Acknowledgments

F.G-G. is funded by the Spanish Ministerio de Ciencia, Innovación y Universidades, the Agencia Estatal de Investigación and EC FEDER funds under project RTI2018-100920-J-I00. MALV, AB, AM, and AS were supported by grant PGC2018-101836-B-100 (MCIU / AEI / FEDER, EU). The IAA team acknowledges financial support from the State Agency for Research of the Spanish MCIU through the “Center of Excellence Severo Ochoa" award to the Instituto de Astrofísica de Andalucía (SEV-2017-0709)

References

Belyaev, D. A., Fedorova, A. A., Trokhimovskiy, A., Alday, J., Montmessin, F., et al. (2021). Revealing a high water abundance in the upper mesosphere of Mars with ACS onboard TGO. Geophysical Research Letters, 48, e2021GL093411. doi:10.1029/2021GL093411

Brines, A., López-Valverde, M.A., Stolzenbach, A., Modak, A., Funke, B., et al. (2022). Water vapor vertical distribution on Mars during perihelion season of MY34 and MY35 with ExoMars-TGO/NOMAD observations. Paper submitted to JGR-Planets.

Bougher, S. W., Roeten, K.J., Olsen, K., Mahaffy, P.R., Benna, M., et al. (2017), The structure and variability of Mars dayside thermosphere from MAVEN NGIMS and IUVS measurements: Seasonal and solar activity trends in scale heights and temperatures, J. Geophys. Res. Space Physics, 122, 1296-1313, doi:10.1002/2016JA023454.

Forget, F., F. Montmessin, J.-L. Bertaux, F. González-Galindo, S. Lebonnois, et al. (2009), Density and temperatures of the upper Martian atmosphere measured by stellar occultations with Mars Express SPICAM, J. Geophys. Res., 114, E01004, doi:10.1029/2008JE003086.

Gagné, M.-È., J.-L. Bertaux, F. González-Galindo, S. M. L. Melo, F. Montmessin, & K. Strong (2013). New

nitric oxide (NO) nightglow measurements with SPICAM/MEx as a tracer of Mars upper atmosphere circulation and comparison with LMD-MGCM model prediction: Evidence for asymmetric hemispheres, J. Geophys. Res. Planets, 118, 2172{2179, doi:10.1002/jgre.20165

González-Galindo, F., Määttänen, A., Forget, F., & Spiga, A., (2011). The martian mesosphere as revealed by CO_2 cloud observations and General Circulation Modeling, Icarus, 216, 10-22, doi:10.1016 / j.icarus.2011.08.006

González-Galindo, F., López-Valverde, M. A., Forget, F., García-Comas, M., Millour, E., & Montabone, L. (2015). Variability of the Martian thermosphere during eight Martian years as simulated by a ground-to-exosphere global circulation model, J. Geophys. Res. Planets, 120, 2020-2035, doi:10.1002/2015JE004925.

Gröller, H., Montmessin, F., Yelle, R. V., Lefèvre, F., Forget, F., et al. (2018). MAVEN/IUVS stellar occultation measurements of Mars atmospheric structure and composition. Journal of Geophysical Research: Planets, 123, doi:10.1029/2017JE005466

López-Valverde, M.A., Funke, B., Brines, A., Stolzenbach, A., Modak, A., et al. (2022). Martian atmospheric temperature and density profiles during the 1st year of NOMAD/TGO solar occultation measurements. Paper submitted to JGR-Planets.

Määttänen, A., Montmessin, F., Gondet, B., Scholten, F., Hoffmann, H., et al. (2010). Mapping the mesospheric CO_2 clouds on Mars: MEx / OMEGA and MEx / HRSC observations and challenges for atmospheric models, Icarus, 209, 452-469, doi:10.1016/j.icarus.2010.05.017

McCleese, D. J., Heavens, N.G., Schofield, J.T., Abdou, W.A., Banfield, J.L., et al. (2010), Structure and dynamics of the Martian lower and middle atmosphere as observed by the Mars Climate Sounder: Seasonal variations in zonal mean temperature, dust, and water ice aerosols, J. Geophys. Res., 115, E12016, doi:10.1029/2010JE003677.

Modak, A., López-Valverde, M.A., Brines, A., Stolzenbach, A., Funke, B., et al. (2022). Retrieval of Martian atmospheric CO vertical profiles from NOMAD observations during the 1st year of TGO operations. Paper submitted to JGR-Planets.

Montabone, L., Spiga, A., Kass, D. M., Kleinböhl, A., Forget, F., & Millour, E. (2020). Martian Year 34 Column Dust Climatology from Mars Climate Sounder Observations: Reconstructed Maps and Model Simulations. J. Geophys. Res. - Planets, 125, e2019JE006111. doi:10.1029/2019JE006111.

Montmessin, F., Korablev, O., Lefèvre, F., Bertaux, J.-L., Fedorova, A., et al. (2017). SPICAM on Mars Express: A 10 year in-depth survey of the Martian atmosphere, Icarus, 297, 195-216, doi:10.1016/j.icarus.2017.06.022.

Navarro, T., Madeleine, J.-B., Forget, F., Spiga, A., Millour, E., Montmessin, F., & Määttänen, A. (2014). Global climate modeling of the Martian water cycle with improved microphysics andadiatively active water ice clouds. Journal of Geophysical Research (Planets) 119, 1479-1495, doi.org:10.1002/2013JE004550

Savijarvi, H., McConnochie, T.H., Harri, A.-M., & Paton, M. (2019). Water vapor mixing ratios and air temperatures for three martian years from Curiosity, Icarus, 326, 170-175, doi:10.1016/j.icarus.2019.03.020

Schneider, N. M., Milby, Z., Jain, S. K., González-Galindo, F., Royer, E., et al. (2020). Imaging of Martian circulation patterns and atmospheric tides through MAVEN/IUVS nightglow observations. Journal of Geophysical Research: Space Physics, 125, e2019JA027318. doi:10.1029/2019JA027318

Smith, M.D., Interannual variability in TES atmospheric observations of Mars during 1999{2003 (2004). Icarus, 167, 148-165, doi:10.1016/j.icarus.2003.09.010.

Vals, M., Rossi, L., Montmessin, F., Lefèvre, F., González-Galindo, F., et al. (2022). Improved modeling of Mars' HDO cycle using a Mars' Global Climate Model. Paper submitted to JGR-Planets

Vandaele, A.C., Korablev, O., Daerden, F. et al. (2019). Martian dust storm impact on atmospheric H_2O and D/H observed by ExoMars Trace Gas Orbiter. Nature 568, 521{525, doi:10.1038/s41586-019-1097-3